Consequences of eye movements for spatial selectivity

Janis Intoy[1,2*], Yuanhao H. Li[1,2*], Norick R. Bowers[3], Jonathan D. Victor[4], Martina Poletti[1,2], and Michele Rucci[1,2,5,6**]

[1]Center for Visual Science, University of Rochester, Rochester, NY, USA
[2]Department of Brain and Cognitive Sciences, University of Rochester, Rochester, NY, USA
[3]Department of Psychology, Justus-Liebig University, Giessen, Germany.
[4]Feil Family Brain and Mind Research Institute, Weill Cornell Medical College, New York City, NY, USA
[5]Twitter: @aplabUR
[6]Lead Contact
[*]Equal contribution
[**]Correspondence: mrucci@ur.rochester.edu

Summary. What determines spatial tuning in the visual system? Standard views rely on the assumption that spatial information is directly inherited from the relative position of photoreceptors and shaped by neuronal connectivity[1,2]. However, the human eyes are always in motion during fixation[3–6], so that retinal neurons receive temporal modulations that depend on the interaction of the spatial structure of the stimulus with eye movements. It has long been hypothesized that these modulations might contribute to spatial encoding[7–12], a proposal supported by several recent observations[13–16]. A fundamental, yet untested, consequence of this encoding strategy is that spatial tuning is not hard-wired in the visual system, but critically depends on how the fixational motion of the eye shapes the temporal structure of the signals impinging onto the retina. Here we use high-resolution techniques for eye-tracking[17] and gaze-contingent display control[18] to quantitatively test this distinctive prediction. We examined how contrast sensitivity, a hallmark of spatial vision, is influenced by fixational motion, both during normal active fixation and when the spatiotemporal stimulus on the retina is altered to mimic changes in fixational control. We show that visual sensitivity closely follows the strength of the luminance modulations delivered within a narrow temporal bandwidth, so that changes in fixational motion have opposite visual effects at low and high spatial frequencies. By identifying a key role for oculomotor activity in spatial selectivity, these findings have important

implications for the perceptual consequences of abnormal eye movements, the sources of perceptual variability, and the function of oculomotor control.

Keywords: Visual perception; retina; ganglion cell; eye movements; ocular drift; microsaccade; contrast sensitivity.

Results and Discussion

Like many species, humans continually move their eyes during the acquisition of visual information (Figure 1A). Even when attending to a single point, a persistent eye motion—known as ocular drift or eye jitter—incessantly sweeps the image on the retina, stimulating photoreceptors with luminance transients rich in spatial information (Figure 1B,C). Several observations including neuronal sensitivity to small input changes[19–23], perceptual impairments in the absence of eye movements[13–15], and considerations of computational efficiency[24,25], support the proposal that the visual system uses these temporal modulations for processing spatial information[7,8,10–12].

Despite the increasing recognition that eye movements contribute to visual encoding, it remains commonly assumed that spatial selectivity in the visual system is primarily the outcome of spatial factors, such as the distribution of specific cell types and their interconnections[1,2,26–29]. However, a spatiotemporal encoding strategy makes the fundamental and distinguishing prediction that spatial selectivity is not just determined by these elements, but critically depends on how eye movements package spatial information in the temporal flow impinging onto the retina[30]. Here we test this hypothesis by examining how one of the most fundamental and widely investigated functions of spatial vision, contrast sensitivity, is affected by the systematic and predictable way in which temporal signals vary with the amount of fixational jitter.

Our driving hypothesis is that sensitivity depends on strength of the fixational luminance fluctuations resulting from eye drifts. To obtain quantitative predictions, we modeled ocular

drift as a Brownian Motion process. This model accounts for the main characteristics of the fixational motion of the eye[24,31] and conveniently summarizes its extent with a single parameter: the diffusion constant, the rate by which the variance of eye displacement increases over time. As shown in Figure 1D,E, varying this value changes the temporal structure of the resulting luminance modulations, as it affects the proportion of power in the stimulus that ocular drift makes available in the form of luminance fluctuations. This quantity, which we will refer to as temporal power, defines the amplitude of fixational modulations across temporal frequencies. As the diffusion constant increases, the external image (in this example a grating at 16 cycle/deg) is transformed onto the retina into modulations at increasingly higher temporal frequencies.

This phenomenon is more comprehensively described by Figure 1F, which shows the power redistribution resulting from ocular drift—as in the two examples of Figure 1E—as the diffusion constant varies systematically. Note that the power delivered at individual temporal frequencies (the sections marked by triangles in Figure 1F) peaks at progressively higher diffusion constants as temporal frequency increases (Figure 1G). Thus, changes in fixational motion are expected to modulate the efficacy of input signals in driving visual responses, as they alter the strength of the signal within the temporal bandwidth of visual sensitivity.

This input reformatting enables formulation of quantitative predictions about the impact of eye movements. If indeed sensitivity relies on fixational modulations, we would expect it to follow the power released at non-zero temporal frequency, peaking for a motion amount that maximizes the total power delivered within the temporal bandwidth effective in eliciting responses. This prediction contrasts with those of traditional views arguing for purely spatial mechanisms in constraining spatial selectivity. Those views would predict sensitivity to either (a) progressively decline with increasing amount of motion (as the black curve in Figure 1G), if spatial processing relies on the stationary image on the retina and discards fixational fluctuations; or (b) to remain largely unaffected by the characteristics of motion if the visual system uses fixational modulations of luminance to simply "refresh" neural activity,

embodying the widespread notion that small motion—irrespective of its characteristics—enhances sensitivity to the image on the retina.

[Figure 1 about here]

To test these predictions, we asked human observers to report whether a grating was tilted clockwise or counterclockwise ($\pm 45°$), while the motion of the stimulus on the retina was controlled via gaze-contingent display. Using a custom apparatus for updating the display in real-time according to high-resolution measurements of eye movements[17,18], we moved the stimulus proportionally to the ongoing gaze shift, $\Delta\mathbf{e}$: $\Delta\mathbf{x} = \gamma\Delta\mathbf{e}$, where γ represents the stabilization gain (Figure 2*A*). When $\gamma = 0$, the image was stationary on the monitor so that the stimulus moved normally on the retina because of the natural eye drift. When $\gamma = 1$, the stimulus moved with the eye to keep the image fully stabilized on the retina. Similarly, gains between 0 and 1 and negative gains respectively attenuated and amplified retinal image motion. Only trials in which the stimulus moved solely because of fixational drift (no saccades or microsaccades) were considered in this study.

Previous studies have indicated that the stimulus within the fovea influences ocular drift[5,15,32–35], In our experiments, to maintain the quality of retinal stimulation consistent and equalize possible extraretinal influences, special care was taken to minimize changes in eye movements across gain conditions. This was achieved by presenting a high frequency stimulus (a 16 cycle/degree grating, as in Figure 1D), while preventing foveal stimulation by means of an artificial scotoma, a retinally stabilized gray patch with diameter of 1 degree. Off-line examination of recorded oculomotor traces confirmed that this approach was effective in maintaining uniform statistics of eye movements across gains (Figure S1) and that the amount of retinal motion varied with the gain parameter as expected (Figure 2*B*), thus confirming that eye movements did not compensate for the altered stabilization gain. Deviations from perfect oculomotor compensation (dashed line in Figure 2*B*) were only visible for the case of full retinal stabilization ($\gamma = 1$), where small measurement errors around $1'$ and

delays in the apparatus (typical delay 7.5 ms) unavoidably prevented perfect immobilization of the stimulus on the retina.

Contrast sensitivity varied greatly with the stabilization gain, yielding a non-monotonic pattern that peaked under conditions of normal retinal motion (Figure 2*C*). Compared to normal viewing, sensitivity fell by approximately 10% with attenuated motion and by 34% when fully stabilized on the retina (p = 0.0351, Tukey's HSD post-hoc test). Increasing retinal image motion also had a negative impact. Sensitivity was comparable to the level measured under full stabilization when retinal image motion was doubled relative to normal (γ=-1; a reduction of ∼30%), and it dropped even more when motion was further amplified, resulting in an average reduction of 56% with γ=-2 (p = 0.0002, Tukey's HSD post-hoc test). Thus, performance is highest with normal fixational motion and deteriorates when the retinal motion is either increased or attenuated. This effect cannot be explained by a varying degree of visuomotor contingency (i.e., the consistency between eye movements and retinal motion) across gain conditions: the same pattern of results was also obtained in control experiments in which retinal motion was varied while ensuring that there was always no consistency between the visual input and oculomotor activity (see Supplementary Figure S2).

[Figure 2 about here]

To inquire into the mechanism responsible for these results, we examined how contrast sensitivity varies with the strength of the luminance modulations resulting from eye movements. To this end, Figure 3*A* replots the contrast sensitivity measurements as a function of the diffusion constant of retinal motion. As shown by these data, motion attenuation and amplification are not equivalent in their perceptual influences. Sensitivity falls sharply when retinal image motion is less than normal, as shown by the strong perceptual impairment observed under full retinal stabilization (a reduction in the motion diffusion constant by ∼10 arcmin^2/s). In contrast, amplification of fixational motion appears to have a more gradual

influence, and the diffusion constant had to be increased by more than 40 arcmin^2/s to produce an impairment comparable to that resulting from full stabilization.

Interestingly, the way sensitivity changes as a function of the amount of retinal motion closely follows the strength of the visual signals delivered by fixational modulations in an intermediate range of temporal frequencies (the inverse u-shaped curves in Figure 1*G*). To provide a qualitative comparison, these curves are re-plotted normalized by their peaks in Figure 3*A* (red curves). A more quantitative analysis is given in Figure 3B, which reports the proportion of variance in sensitivity across gain conditions (the coefficient of determination R^2) that is explained by the luminance fluctuations at any given temporal frequency (the abscissa in Figure 3B). As shown by these data, sensitivity is well predicted by the strength of the luminance modulations delivered in a narrow frequency band around 5 Hz.

Neurons in the retina are known to respond strongly to temporal changes. Figure 3*C* compares perceptual measurements to the estimated efficacy of fixational modulations in driving the responses of parvocellular ganglion cells, the neurons that are likely to respond to the high spatial frequency of the stimulus used in our experiments. The red curve in Figure 3*C* represents the total power made available by the motion of the eye in form of changes in luminance—*i.e.*, the power delivered at non-zero temporal frequencies—integrated by the temporal sensitivity of parvocellular neurons, as reported in the neurophysiological literature[36]. The similarity between this input signal and psychophysical measurements is striking, particularly considering that the comparison is parameter-free. A direct comparison between psychophysical data and the strength of fixational modulations is provided in Figure 3D. Performance and power are not only very strongly correlated ($r(33) = 0.81$, $p < 0.001$), they also appear to be nearly proportional: the slope of the power-law regression is 0.86, with a confidence limit that includes 1 (Figure 3D). Thus, the temporal power delivered by fixational modulations is a good predictor of how contrast sensitivity changes with the amount of motion.

[Figure 3 about here]

The results presented so far lead to an intriguing hypothesis. Ocular drift is known to vary naturally across fixations, at times moving the eyes more and in other occasions keeping gaze narrowly centered. As shown in Figure 1, these movements result in different reformatting of spatial patterns into luminance modulations on the retina. Since the data in Figure 3 show that visual sensitivity varies with temporal power, the hypothesis emerges that the physiological variability in fixational control may contribute to trial-to-trial fluctuations in performance during assessments of visual functions[37–39].

This hypothesis can be made more specific by considering how the oculomotor reformatting of visual input signals varies with the spatial characteristics of the stimulus. The consequence of a change in the amount of fixational motion critically depends on the spatial frequency of the stimulus. This effect is shown in Figure 4*B* for the Brownian model of fixational motion. The two curves represent the strengths of fixational luminance modulations—the input signal filtered by the temporal sensitivity of the visual system[40]—as a function of the motion diffusion constant during viewing of gratings at either low (0.8 cycle/deg) or high spatial frequency (10 cycles/deg). An increment in the amount of motion has opposite effects on the power of fixational modulations delivered by these two stimuli. A larger motion yields a stronger input during exposure to a stimulus of low spatial frequency, as it amplifies luminance modulations (solid line, green arrow). In contrast, a larger fixational motion weakens the visual input for a stimulus of high spatial frequency, as power shifts to temporal frequencies that are beyond the range of visual sensitivity (dashed line, blue arrow). Thus, we would expect an increment in motion to be perceptually beneficial at low spatial frequencies and detrimental at high frequencies.

To test these predictions, we measured performance in a discrimination task similar to the one of the previous experiments. However, rather than manipulate retinal image motion experimentally, we merely tracked spontaneous trial-to-trial variations in eye movements. As

in Figure 2, subjects reported whether a grating was tilted clockwise or counter-clockwise by 45°, but they were here exposed only to the normal motion provided by their fixational drifts (Figure 4*A*). In separate blocks of trials, gratings were either at low (0.8 cycle/deg) or high spatial frequencies (10 cycles/deg) with contrast at their respective threshold levels. To quantify motion variability, we evaluated the motion diffusion constant in each trial and estimated its distribution (Figure 4C). As expected, ocular drift varied considerably through time, yielding considerably different values for trials with diffusion constants in the lower and upper 40^{th} percentiles (Figure 4*D*). Figure 4*E* compares perceptual performance in these two groups of trials. In keeping with the strength of fixational modulations in Figure 4*B*, the amount of motion had a strong influence on performance: a larger movement was beneficial with the low-frequency 0.8 cycles/deg stimulus ($p = 0.027$) but detrimental at 10 cycles/deg ($p = 0.047$, two-tailed, paired t-test). Thus, variations in the amount of motion affect visual sensitivity as predicted by their temporal reformatting of visual input signals.

[Figure 4 about here]

In sum, the results of these experiments confirm the prediction from neural models[30] that eye movements participate in shaping visual sensitivity. This action stems directly from the consequences of eye movements for visual input signals, rather than their associated extraretinal influences[41–45]: by regulating the extent by which luminance modulations fall within the temporal bandwidth of the visual system, the fixational motion of the eye effectively controls the contrast of the stimulus on the retina. Contrary to the traditional notion of a non-specific gain resulting from a global "refreshing" of neural activity, this modulation is not uniform across spatial frequencies, but it respectively enhances sensitivity to lower and higher spatial frequencies when the amount of motion increases or decreases. Our results show that this effect is robust and occurs during both passive exposure to controlled retinal stimulation and during a normally active fixation.

These findings add to a growing body of evidence supporting the idea that spatial vision

relies heavily on the oculomotor-shaped temporal flow of visual information[12,46]. The luminance modulations from ocular drifts[15,16], microsaccades[33], saccades[47], and even eye blinks[48] have all been found to be beneficial in spatial frequency ranges that are consistent with their structure. This scheme of visual encoding is computationally parsimonious, as it assumes common neural mechanisms for operating on luminance transients, irrespective of their origin. The present results go beyond the previous literature by providing direct evidence that visual sensitivity closely follows the spatial information contained in the luminance modulations delivered by eye movements. Specifically, our data show that the previously reported optimal range of temporal sensitivity for externally moving stimuli[49] also seems to be responsible for shaping spatial sensitivity during fixation. Since the amount of fixational eye motion determines how the strength of these temporal signals varies with the spatial frequency of the stimulus, our results show that spatial sensitivity during fixation is not just determined by the spatial tuning properties of neuronal receptive fields, but also by how the eye moves during the acquisition of visual information. Additionally, this finding raises the hypothesis that a portion of the fluctuations in perceptual performance[37–39] can be explained by the trial-to-trial variations in drift trajectories that normally occur during the course of an experiment.

While in this study we have focused on the consequences of fixational eye movements for a system-level property of spatial vision, contrast sensitivity, similar considerations apply to the spatial tuning of individual neurons in the visual pathways departing from the retina. Both in the retina and at later stages of processing, neurons vary in their selectivity to spatial frequency[36,50–53]. Our results predict that selectivity measurements obtained in the presence and absence of eye movements, as in awake and anesthetized preparations, will differ because of the input reformatting resulting from eye movements. Specifically, measurements obtained with limited or altered fixational motion will be influenced by temporal modulations that differ in structure from those caused by a normally active fixation.

These considerations highlight the importance of paying attention to both the spatial and

temporal characteristics of retinal stimulation when evaluating visual functions. In vision research, the temporal properties of the stimulus are often considered of subordinate importance relative to its spatial configuration. However, strong unnatural transients, like abrupt stimulus onsets, yield spatial distributions that differ widely from those experienced during normal viewing, even from saccades[54]. For example, delivering the stimulus by means of a 30-Hz train of flashes, as it happens in scanning laser ophthalmoscopes[55], will yield useful temporal signals even in the absence of eye movements, as the temporal redistribution of power resulting from oculomotor activity gets convolved with the modulation in the stimulus contrast. In these conditions, partial attenuation of retinal image motion is expected to be beneficial (see modeling prediction in Figure S4). This observation has been confirmed experimentally[56], but its implications have been examined without consideration of temporal factors, leading to the conclusion that fixational eye movements are not optimal for vision, an inference that conflicts with the results of Figure 2.

Our findings carry important implications regarding the functions of fixational oculomotor control[32,57–59] and the consequences of abnormal eye movements[60–64]. Since, as we show, spatial selectivity critically depends on the amount of retinal image motion, the hypothesis emerges that task-dependent regulation of retinal motion may be an important goal of fixational control. In this view, the less-rapid eye drifts observed in high-acuity judgements[15,33] could be regarded as the outcome of a control mechanism aimed at shifting selectivity toward higher spatial frequencies. Furthermore, many visual impairments are associated with abnormal fixational stability[63,65–67], which alters the structure of the temporal signals impinging onto the retina. Our results raise not only the hypothesis that changes in the temporal flow of visual stimulation could account for some of the visual impairments observed in these conditions, but also that changes in fixational behavior could stem from attempting to compensate for impaired visual sensitivity. Further work is needed to investigate these emerging hypotheses.

Acknowledgements: This work was supported by grants R01 EY18363, EY07977, EY02788, and P30 EY001319 from the National Institutes of Health. We thank the members of the UR Active Perception Laboratory for helpful discussions.

Author contributions: MP, JV and MR conceived and designed the study. NB, MP and YL implemented the experiments and collected the data. JI and YL analyzed the data. All authors contributed to the interpretation of the results and the writing of the article. MR supervised the project.

Declaration of Interests: The authors declare no competing interest.

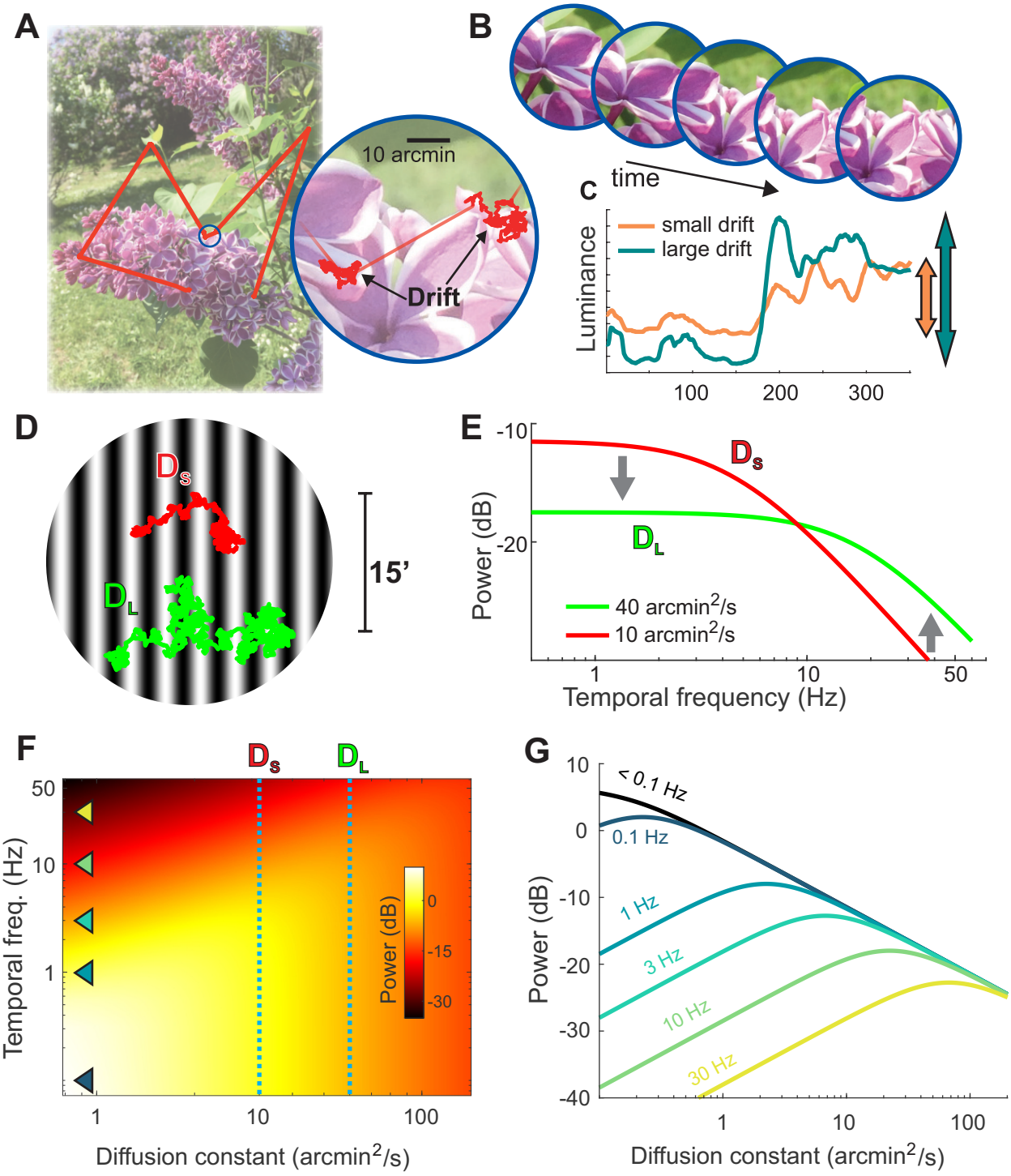
A
10 arcmin
Drift
B
time
C
small drift
large drift
Luminance
100
200
300
D
D_S
D_L
15'
E
-10
-20
D_S
D_L
Power (dB)
40 arcmin^2/s
10 arcmin^2/s
1
10
50
Temporal frequency (Hz)
F
D_S
D_L
50
10
1
Temporal freq. (Hz)
Power (dB)
0
-15
-30
1
10
100
Diffusion constant (arcmin^2/s)
G
10
0
-10
-20
-30
-40
< 0.1 Hz
0.1 Hz
1 Hz
3 Hz
10 Hz
30 Hz
Power (dB)
1
10
100
Diffusion constant (arcmin^2/s)

Figure 1

Figure 1. Visual input during active fixation. **(A-C)** Eye movements continually modulate visual signals to the retina. **(A)** An oculomotor trace superimposed on the observed image. The insert zooms in to show two periods of fixational motion (ocular drifts) separated by a small saccade (microsaccade). **(B)** The spatiotemporal stimulus impinging onto the retina during an intersaccadic period. **(C)** The luminance modulations experienced by an individual photoreceptor for two different amounts of fixational motion. Larger eye drifts tend to yield stronger and faster modulations during viewing of natural scenes. **(D-F)** Consequences of varying the amplitude of the fixational motion. **(D)** Two traces drawn from a Brownian motion (BM) model of ocular drift. In this model, the amount of motion depends on the diffusion constant, a parameter that describes how rapidly the eye moves away from its original position ($D_L = 40$ arcmin^2/s; $D_S = 10$ arcmin^2/s). The stimulus is a 16 cycle/deg grating. **(E)** Fraction of stimulus power that the fixational eye motion makes available at a given temporal frequency on the retina. Increasing the extent of fixational motion yields modulations over a broader range of temporal frequencies. **(F)** Spatio-temporal power redistribution as a function of the diffusion constant. The dashed vertical lines correspond to the two curves in panel E. **(G)** Temporal frequency sections through the power redistribution function (triangles in F). Note that the amount of motion that maximally stimulates the retina varies with temporal frequency sensitivity.

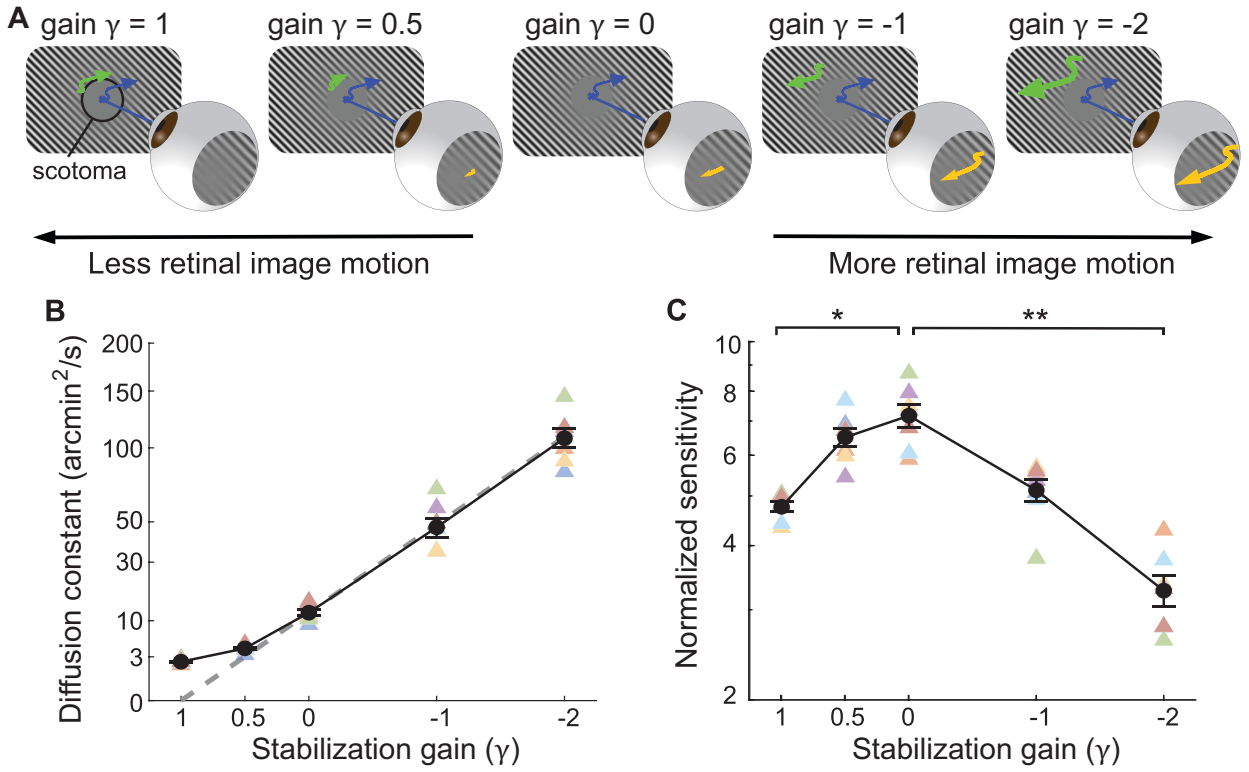

Figure 2: **Influence of fixational motion on visual sensitivity. (A)** Human observers reported the orientation ($\pm 45°$) of a $58° \times 50°$ grating while exposed to the visual input signals resulting from different amounts of fixational motion. This was achieved via gaze-contingent display control, by moving the stimulus on the display (green arrows) following the line of sight (blue arrows) with a range of stabilization gains, γ. Depending on the stabilization gain, the resulting motion on the retina (yellow arrows) was attenuated ($\gamma > 0$) or amplified ($\gamma < 0$) relative to normal ($\gamma = 0$). To minimize changes in eye movements across conditions, a retinally-stabilized gray disk (a 1° diameter artificial scotoma) prevented foveal exposure of the stimulus (a 16 cycles/deg grating). **(B)** This procedure was effective in delivering a desired amount of motion on the retina. The mean estimated diffusion constants of fixational motion (black circles) were close to those expected theoretically assuming perfect compensation and that eye movements are not influenced by the gain (dashed line; see also Figure S1). Black circles and error bars represent average values and $\pm$ one SEM across subjects ($N = 7$). Colored triangles are the data from individual subjects. **(C)** Dependence of contrast sensitivity on the stabilization gain. Data points represent changes relative to each subject's individual sensitivity, averaged across conditions. Graphical conventions are as in B. Sensitivity was impaired when retinal image motion was attenuated or amplified ($^{*}p = 0.0351$ and $^{**}p = 0.0002$ respectively, Tukey's HSD post-hoc tests). See also Figure S2.

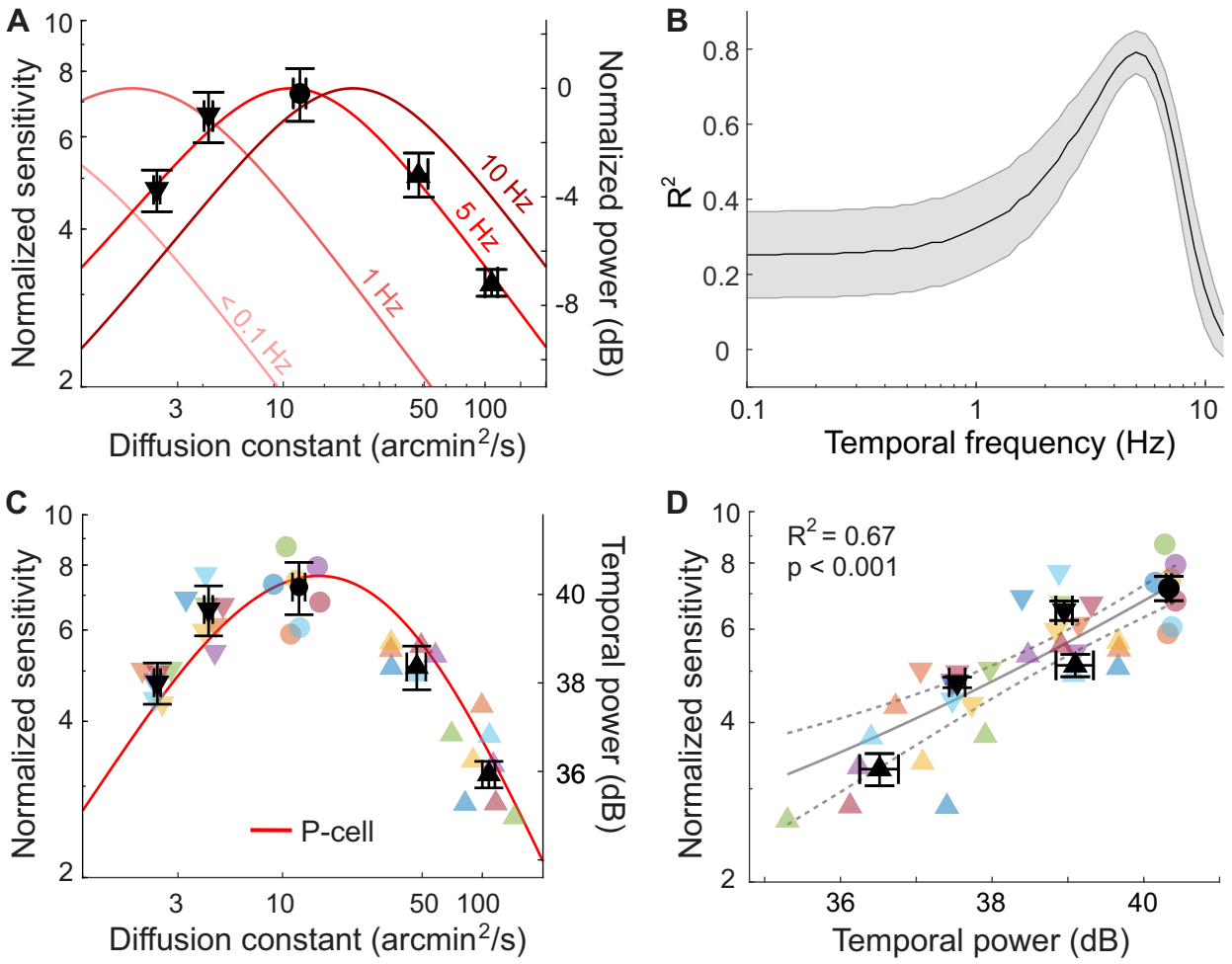

Figure 3: **Fixational luminance modulations predict visual sensitivity.** **(A-B)** Comparing psychophysical data to the consequences of input reformatting resulting from fixational motion. **(A)** Average contrast sensitivity measurements (left ordinate; same data as in Figure 2C), now reported as a function of the diffusion constant of retinal motion (abscissa). The red curves (right ordinate) show the power distributions of fixational luminance modulations at individual temporal frequencies (the curves in Figure 1G, normalized by their peaks). Note that sensitivity data well align with the power available at 5 Hz. **(B)** Coefficient of determination in fitting contrast sensitivity measurements with the spectral density functions at individual temporal frequencies. Data are well predicted by the power in a narrow frequency band. The shaded gray region represents ± one standard error. **(C-D)** Comparing psychophysical data to the strength of the visual input effective in driving retinal neurons. **(C)** The same data as in *A* now plotted together with the strength of the input signal delivered within the range of sensitivity of a parvocellular neuron (the integrated power weighted by the cell's temporal sensitivity[36], right ordinate). **(D)** Direct comparison between contrast sensitivity and the effective input to a model parvocellular cell. Solid gray and dashed lines show linear regression (slope 0.86) and 95% confidence intervals (0.64-1.07), respectively (see also Figure S3). In *A*, *C*, and *D*, filled black symbols and error bars represent averages and standard errors across subjects for each gain condition. Colored symbols are data from individual subjects. Symbol shapes indicate whether retinal image motion was attenuated ($\gamma > 0$; downward triangles), amplified ($\gamma < 0$; upward triangles) or unchanged ($\gamma = 0$; circles). See also Figure S4.

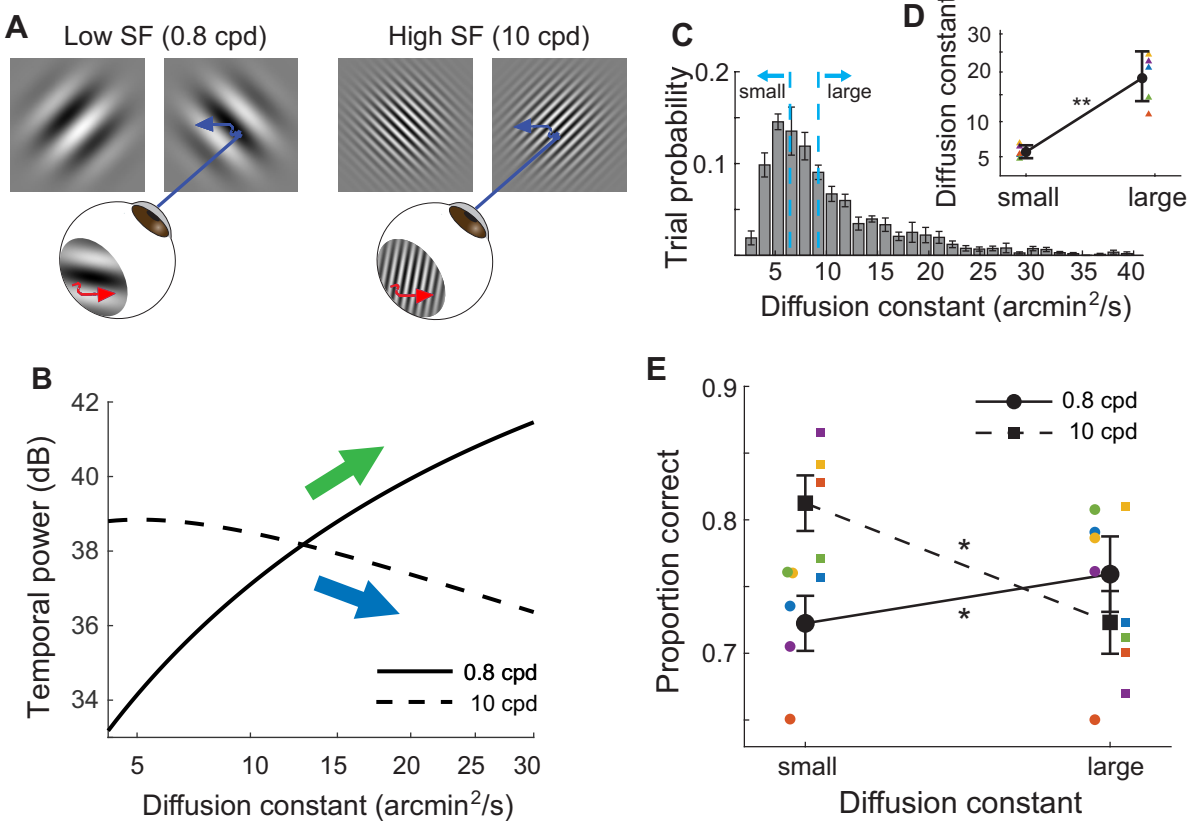

Figure 4: **Visual consequences of the physiological variation in fixational motion.** **(A)** Subjects (N=5) reported the orientation (±45°) of a grating (spatial frequency: 0.8 or 10 cycles/deg) during normal fixation. The stimulus contrast was adjusted for each individual subject to yield ∼75% correct responses. **(B)** Strength of fixational modulations (the input power filtered by temporal visual sensitivity[40]) as a function of the diffusion constant of motion. A Brownian Motion model of ocular drift predicts that varying the amount of fixational motion yields opposite effects during viewing of stimuli at low and high spatial frequencies. **(C)** Natural trial-to-trial variation in fixational motion for one subject. The histogram represents the distribution of the motion diffusion constants estimated in individual trials. **(D)** The mean diffusion constants for trials in the bottom and top 40^{th} percentiles (small and large trials, respectively; blue dashed lines in C) differ considerably. Error bars represent ± one standard deviation. Triangles are data from individual subjects. **(E)** Proportion of correct responses in the two groups of trials. Increasing the amount of motion is beneficial at low and detrimental at high spatial frequency ($^*p = 0.027$ and 0.047 respectively; two-tailed paired t-tests. $N = 5$). Black symbols and error bars represent means and SEM across subjects. Colored symbols are data from individual subjects.

STAR Methods

Resource Availability

Lead Contact. Further information and requests for resources should be directed to and will be fulfilled by the Lead Contact, Michele Rucci (mrucci@ur.rochester.edu).

Materials availability. This study did not generate new unique reagents.

Data and code availability.

- The dataset generated in this study have been deposited to Mendeley Data: https://doi.org/10.17632/pnyjrd93s7.1 and is publicly available as of the date of publication.
- This study used standard programmed scripts developed in MATLAB that are available from the lead contact upon request.
- Any additional information required to reanalyze the data reported in this paper is available from the lead contact upon request.

Experimental model and study participant details

Human Subjects

Twelve naïve subjects (9 females and 3 males; age range: 21-31 years) took part in the study, 7 in the controlled motion experiments of Figs. 2-3, 5 in the experiment of Figure 4, and 3 in the experiments of Figure S2. All subjects possessed uncorrected 20/20 vision, tested by a standard Snellen eye-chart, and were compensated for their participation. Informed consent was obtained from all participants following the procedures approved by the University of Rochester and the Boston University Charles River Campus Institutional Review Board.

Method details

Stimuli and Apparatus

Stimuli consisted of large-field sinusoidal gratings (Figure 2 and Figure S2) or Gabor patches (Figure 4) tilted by ±45° relative to the vertical axis and displayed over a uniform background (luminance 7 cd/m^2; field size: 58° by 50°). In the controlled motion experiments (Figure 2), the grating was 16 cycles/deg and foveal vision was eliminated by an artificial scotoma to minimize the possibility that eye movements would change with the stabilization gain. The artificial scotoma was a circular (1° diameter) opaque gray region at background luminance with a surrounding 0.5° annulus of tapered transparency, which remained centered on the line of sight as the eyes moved normally during fixation. Gabor patches had a frequency of either 0.8 or 10 cycles/deg and a Gaussian envelope with standard deviation of 2.25°.

Stimuli were displayed on a gamma-corrected fast-phosphor CRT monitor in the experiments of Figs. 2- 4 (Iiyama HM204DT; refresh rate: 200 Hz) or an LCD monitor in the experiment of Figure S2 (Asus Rog Swift PG259QN; refresh rate: 360 Hz) in a dimly illuminated room. Stimuli were viewed monocularly with the right eye while the left eye was patched. The subject's head was immobilized by a dental imprint bite-bar and a headrest to maintain a fixed distance of 123 cm from the monitor. Movements of the viewing eye were measured by Dual Purkinje Image (DPI) eye-trackers, either the commercial analog device (Fourward Technologies) or a custom digital version[17]. Stimuli were rendered using EyeRIS, a system for gaze-contingent display control that enables real-time synchronization between oculomotor measurements and the updating of the image on the monitor[18]. The average delay of stimulus updating in these experiments was 7.5 ms (maximum delay 10 ms).

Data collection

Data were collected in multiple experimental sessions, each lasting approximately 1 hour. Within each session, 10-15 minute blocks of trials were separated by brief breaks in which the subject was allowed to exit the apparatus and rest. Every session started with preliminary

procedures aimed at ensuring optimal eye-tracking and gaze-contingent control. Precise spatial registration between eye movements and the stimulus on the monitor was obtained by a two-step calibration procedure that mapped oculomotor signals from the DPI into display coordinates[68]. In this procedure, the mapping obtained by means of a standard 3×3 grid was refined in a second gaze-contingent phase, in which subjects manually corrected possible offsets in the estimated position of gaze, now displayed in real time on the monitor. This correction was performed using a joypad while fixating on each point of the calibration grid. To counteract possible misalignments caused by drifts in the apparatus or minute head movements, this gaze-contingent refinement was repeated for the central grid point every 5 trials.

Perceptual task

In a forced-choice procedure, subjects reported whether the grating was tilted to the left or to the right. The orientation of the stimulus varied randomly across trials. Each trial started with the subjects fixating for 500 ms on a marker (a 10′ dot) at the center of a uniform gray field. The stimulus then appeared gradually with linearly increasing contrast over an initial period (800 ms in Figure 2, 500 ms in Figure 4), which was followed by 500 ms exposure at the plateau contrast. A large-field maximum contrast noise mask ended the trial, prompting subjects to report the perceived orientation of the grating by pressing one of two buttons on a joypad. The contrast of the grating varied adaptively across trials following the Parametric Estimation by Sequential Testing (PEST) procedure[69] aiming for ∼75% correct discrimination for each individual.

In the experiments of Figure 2 and Figure S2, the gain γ of retinal stabilization was varied systematically to control retinal motion[56,70,71]. That is, as the eye moved by $\boldsymbol{\Delta e}$, the stimulus also moved on the display by $\boldsymbol{\Delta s} = \gamma \boldsymbol{\Delta e}$. Consequently, the stimulus remained immobile on the monitor for $\gamma = 0$ (normal viewing) and immobile on the retina for $\gamma = 1$ (full retinal stabilization). Gain values between zero and 1 decreased the amount of retinal image

motion, whereas negative γ amplified retinal image motion by moving the stimulus in the opposite direction of the eye, so that, on the retina, it moved in the direction consistent with normal viewing, but over a larger distance. The gain varied randomly across blocks of trials, taking values of 1, 0.5, 0, -1, and -2. In Supplementary Figure S2, the stimulus always moved on the display to fully compensate for the subject's eye movements, while a previously recorded oculomotor trace was superimposed to this motion and scaled by a desired gain. In each trial, the superimposed trace was randomly selected from a database of ocular drift recordings collected while the subject maintained fixation. This approach enabled control of the amount of retinal image motion while eliminating visuomotor contingencies.

Quantification and statistical analysis

Psychophysical performance

Contrast thresholds reported in this study represent the contrast values yielding 75% correct discrimination. Thresholds were estimated by using all tested contrast levels and modeling psychometric functions with cumulative log-normal curves via the maximum likelihood procedure proposed by [72]. Contrast sensitivity was defined as the inverse of the estimated contrast threshold. The mean sensitivity data reported in Figure 2 and 3 represent averages across subjects after normalizing each individual by their average sensitivity across all gains. In Figure 4, only trials with stimulus contrast close to the 75% threshold were considered. To ensure reliable estimation of diffusion constants, performance was then evaluated over the pools of trials in which the eye moved considerably more or less than average.

Oculomotor data

Analog eye movement traces were first low-pass filtered at 500 Hz and then sampled at 1 kHz together with binary signals marking blinks and periods of no-tracking, which were automatically detected by the eye-tracker. The digital DPI directly provided time series sampled at 1 kHz. The sampled oculomotor traces were then segmented into periods of

saccades and drifts by means of a speed threshold of 2°/s as previously described[15]. In this study we only considered the trials in which the eye moved exclusively because of ocular drift. All trials containing blinks, saccades or microsaccades during stimulus presentation were discarded from data analysis. Instantaneous speed and curvature of the recorded traces were estimated after low-pass filtering oculomotor data with a Savitzky–Golay filter with cut-off frequency at approximately 40 Hz. The diffusion constants of the equivalent Brownian motion processes were estimated as described below for the retinal trajectories.

Retinal input

For each trial, we reconstructed the trajectory followed by the stimulus on the retina by subtracting the position of the image on the monitor from the estimated position of the line of sight. These traces were synchronized and saved at the end of each trial by EyeRIS, our apparatus for gaze-contingent display control. In the case of normal viewing, (stabilization gain $\gamma = 0$) the retinal trajectory was identical to the eye drift trace.

We modeled the resulting fixational motion as a Brownian diffusion process. In this model, the probability of displacement $[\Delta x, \Delta y]$ after any given interval Δt follows a normal distribution:

$$q(\Delta x, \Delta y, \Delta t) = \frac{1}{4\pi D \Delta t} \exp\left(-\frac{\Delta x^2 + \Delta y^2}{4D\Delta t}\right)$$

where the diffusion constant D determines the rate by which the displacement variance increases over time, $\sigma^2(t) = 4D\ \Delta t$. This model has been previously shown to well account for the characteristics of ocular drifts[24,73,74]. It also well approximated the retinal motion signals measured with stabilization gains $\gamma \neq 0$, all of which exhibited approximately linearly increasing variances with time. For each subject and stabilization gain, we estimated the diffusion constant D_γ via linear regression of $\sigma^2_\gamma(t)$ using the traces recorded during the plateau period of stimulus presentation. The estimated D_γ increased in proportion to $(1-\gamma)^2$ (the dashed line in Figure $2B$), which is the expected behavior in the ideal case of perfect retinal stabilization and unchanged eye movements across conditions.

Spectral analyses

The Fourier Transform of the probability distribution of gaze displacement, $q(\Delta x, \Delta y, \Delta t)$, defines the proportion of power in the stimulus that the fixational motion redistributes across temporal frequencies[24]. A Brownian motion model enables a closed form estimation of this redistribution:

$$Q(\mathbf{k}, \omega) = \frac{2D|\mathbf{k}|^2}{D^2|\mathbf{k}|^4 + \omega^2} \tag{1}$$

where $\mathbf{k} = (k_x, k_y)$ and ω represent spatial and temporal frequency, respectively.

For every spatial frequency $\mathbf{k}$, the function Q can be regarded as the power spectrum of the spatiotemporal flow of luminance delivered by a grating with fixed contrast (unit power). In our experiments, however, to minimize temporal transients from sources other than the motion of the eye, the power of the grating varied through time, as its contrast slowly ramped up at the beginning of each trial before reaching a plateau. This temporal modulation spreads the power of the stimulus across temporal frequencies even in the absence of retinal motion, an operation that corresponds to a convolution in the Fourier domain. As a consequence, the power spectrum of the stimulus on the retina is given by:

$$P(\mathbf{k}, \omega) = |P_S(\omega)|^2 *_\omega Q(\mathbf{k}, \omega) \tag{2}$$

where $\star_\omega$ indicates temporal convolution and P_S is the Fourier Transform of the contrast profile:

$$P_S(\omega) = \frac{2 + \omega^2 T_0^2 - 2\cos(\omega T_0) - 2\omega T_0 \left[\sin(\omega(T_0 - T_1)) + \sin(\omega T_1)\right]}{\omega^4 T_0^2}$$

with T_0 and T_1 representing the durations of the contrast ramp and plateau periods, respectively. In the analyses of Figure 3, we used Eq. 2 to estimate the power spectrum of the visual input signal experienced by every subject in every gain condition. This signal varied across subjects because of their individual eye movements and how well they were

compensated by our apparatus.

Relating visual signals to performance

We examined the relation between visual sensitivity and the strength of the luminance modulations resulting from the fixational motion on the retina. To this end, we asked whether a specific range of temporal frequencies exists for which variations in sensitivity across gain conditions correlate with the visual input power made available by the fixational motion. Figure 3B reports the amount of variance in sensitivity that is explained by the power of fixational fluctuations (estimated from Eq. 2) as a function of temporal frequency.

To estimate the efficacy of the fixational visual flow in driving perceptual and neural responses, we computed the total strength of the resulting signal within the temporal range of sensitivity of the visual system and the retina. This signal provides a direct measure of the response of a linear model. To this end, spectral distributions were weighted by a temporal sensitivity function H and integrated across all non-zero temporal frequencies:

$$P_{\gamma}^{TOT}(\mathbf{k}) = \int_{0+}^{\infty} P_{\gamma}(\mathbf{k}, \omega) \cdot |H(\omega)|^2 \, d\omega \tag{3}$$

In Figure 4C-D, to compare the perceptual influences of eye movements on stimuli at low and high spatial frequencies, we used the temporal sensitivity of the human visual system as measured by Kelly (1979) under retinal stabilization ($H = H_K$). These measurements exclude the confounds from fixational eye movements, the effects that we aim to characterize in our study. Following the model proposed by Kelly:

$$H_K(k, \omega) = \left[6.1 + 7.3 \cdot \left| \log(\frac{\omega}{3k}) \right|^3 \right] \omega k \exp\left[-2k(\omega/k + 2)/45.9 \right]$$

where $k = |\mathbf{k}_0|$ is the spatial frequency of the grating.

No similar characterization of human temporal sensitivity under retinal stabilization exists

for the extra-foveal viewing condition of the experiment of Figure 2. Therefore, for the analyses in Figure 3 we used the temporal profile of parvocellular retinal ganglion cells ($H = H_P$), which are the neurons that are likely to respond to the high spatial frequency stimulus presented in these experiments. The temporal frequency sensitivity of a typical neuron was modeled as in [75]:

$$H_P(\omega) = Ae^{-2\pi\imath d}\left(1 - \frac{M_S}{1+\imath\omega\tau_S}\right)\left(\frac{1}{1+\imath\omega\tau_L}\right)^{N_L}$$

This model was originally developed for cat X cells and later shown to well predict also the responses of macaque P and M cells with proper tuning of the parameters[20,36]. Parameters were taken from the neurophysiological literature to model the responses of cells located at approximately 5° of eccentricity[36]: $N_L = 38$, $A = 67.59$, $d = 3.5$, $M_S = 0.62$, $\tau_L = 1.5$, $\tau_S = 29.36$. To account for the attenuation in sensitivity observed in parvo-cellular neurons at low temporal frequencies[19], H_P decreased linearly below 2 Hz.

Figure 3*C-D* directly compares contrast sensitivity measurements to the power of the driving visual input, estimated as in Eq. 3 with $H = H_P$ and averaged across subjects. Linear regressions for each individual subjects are reported in supplementary Figure S3. Our results show that perceptual sensitivity closely follows the strength of the signal delivered within the temporal sensitivity of parvocellular retinal ganglion cells, as measured by neurophysiological experiments.

References

[1] Wandell, B. A. *Foundations of Vision.* (Sinauer Associates, 1995).

[2] Palmer, S. E. *Vision Science: Photons to Phenomenology* (The MIT Press, 1999).

[3] Ratliff, F. & Riggs, L. A. Involuntary motions of the eye during monocular fixation. *J. Exp. Psychol.* **40**, 687–701 (1950).

[4] Barlow, H. B. Eye movements during fixation. *J. Physiol.* **116**, 290–306 (1952).

[5] Steinman, R. M., Haddad, G. M., Skavenski, A. A. & Wyman, D. Miniature eye movement. *Science* **181**, 810–819 (1973).

[6] Kowler, E. Eye movements: The past 25 years. *Vision Res.* **51**, 1457–1483 (2011).

[7] Averill, H. I. & Weymouth, F. W. Visual perception and the retinal mosaic. II. The influence of eye movements on the displacement threshold. *J. Comp. Psychol.* **5**, 147–176 (1925).

[8] Marshall, W. H. & Talbot, S. A. Recent evidence for neural mechanisms in vision leading to a general theory of sensory acuity. In Kluver, H. (ed.) *Biological Symposia—Visual Mechanisms*, vol. 7, 117–164 (Cattel, Lancaster, PA, 1942).

[9] Arend, L. E. Spatial differential and integral operations in human vision: Implications of stabilized retinal image fading. *Psychol. Rev.* **80**, 374–395 (1973).

[10] Ahissar, E. & Arieli, A. Figuring space by time. *Neuron* **32**, 185–201 (2001).

[11] Rucci, M. Fixational eye movements, natural image statistics, and fine spatial vision. *Network: Comp. Neural* **19**, 253–285 (2008).

[12] Rucci, M. & Victor, J. D. The unsteady eye: An information processing stage, not a bug. *Trends Neurosci.* **38**, 195–206 (2015).

[13] Rucci, M., Iovin, R., Poletti, M. & Santini, F. Miniature eye movements enhance fine spatial detail. *Nature* **447**, 852–855 (2007).

[14] Ratnam, K., Domdei, N., Harmening, W. M. & Roorda, A. Benefits of retinal image motion at the limits of spatial vision. *J. Vis.* **17**, 30 (2017).

[15] Intoy, J. & Rucci, M. Finely tuned eye movements enhance visual acuity. *Nat. Commun.* **11**, 1–11 (2020).

[16] Clark, A. M., Intoy, J., Rucci, M. & Poletti, M. Eye drift during fixation predicts visual acuity. *Proc. Natl. Acad. Sci. USA* **119**, 1–10 (2022).

[17] Wu, R.-J. *et al.* High-resolution eye-tracking via digital imaging of Purkinje reflections. *J. Vis.* **23** (2023).

[18] Santini, F., Redner, G., Iovin, R. & Rucci, M. EyeRIS: A general-purpose system for eye movement contingent display control. *Behav. Res. Methods* **39**, 350–364 (2007).

[19] Purpura, K., Tranchina, D., Kaplan, E. & Shapley, R. M. Light adaptation in the primate retina: Analysis of changes in gain and dynamics of monkey retinal ganglion cells. *Visual Neurosci.* **4**, 75–93 (1990).

[20] Benardete, E. A. & Kaplan, E. The dynamics of primate M retinal ganglion cells. *Visual Neurosci.* **16**, 355–368 (1999).

[21] Martinez-Conde, S., Macknik, S. L. & Hubel, D. H. Microsaccadic eye movements and firing of single cells in the striate cortex of macaque monkeys. *Nat. Neurosci.* **3**, 251–258 (2000).

[22] Snodderly, D. M., Kagan, I. & Gur, M. Selective activation of visual cortex neurons by fixational eye movements: Implications for neural coding. *Visual Neurosci.* **18** (2001).

[23] Kagan, I., Gur, M. & Snodderly, D. M. Saccades and drifts differentially modulate neuronal activity in V1: Effects of retinal image motion, position, and extraretinal influences. *Vision Res.* **8** (2008).

[24] Kuang, X., Poletti, M., Victor, J. D. & Rucci, M. Temporal encoding of spatial information during active visual fixation. *Curr. Biol.* **20**, 510–514 (2012).

[25] Aytekin, M., Victor, J. D. & Rucci, M. The visual input to the retina during natural head-free fixation. *J. Neurosci.* **34**, 12701–12715 (2014).

[26] Campbell, F. W. & Green, D. G. Optical and retinal factors affecting visual resolution. *J. Physiol.* **181**, 576–593 (1965).

[27] Hirsch, J. & Curcio, C. A. The spatial resolution capacity of human foveal retina. *Vision Res.* **29**, 1095–101 (1989).

[28] Reid, R. C. & Alonso, J. M. The processing and encoding of information in the visual cortex. *Curr. Opin. Neurobiol.* **6**, 475–480 (1996).

[29] Rossi, E. A. & Roorda, A. The relationship between visual resolution and cone spacing in the human fovea. *Nat. Neurosci.* **13**, 156–157 (2010).

[30] Casile, A., Victor, J. D. & Rucci, M. Changes in contrast sensitivity reveal an oculomotor strategy for temporally encoding space. *Elife* **8**, 1–16 (2019).

[31] Cherici, C., Kuang, X., Poletti, M. & Rucci, M. Precision of sustained fixation in trained and untrained observers. *J. Vis.* **12**, 1–16 (2012).

[32] Epelboim, J. & Kowler, E. Slow control with eccentric targets: Evidence against a position-corrective model. *Vision Res.* **33**, 361–380 (1993).

[33] Shelchkova, N., Tang, C. & Poletti, M. Task-driven visual exploration at the foveal scale. *Proc. Natl. Acad. Sci. USA* **116**, 5811–5818 (2019).

[34] Malevich, T., Buonocore, A. & Hafed, Z. M. Rapid stimulus-driven modulation of slow ocular position drifts. *Elife* **6**, e57595 (2020).

[35] Lin, Y., Intoy, J., Clark, A. M., Rucci, M. & Victor, J. D. Cognitive influences on fixational eye movements. *Curr. Biol.* **33**, 1606–1612 (2023).

[36] Benardete, E. A. & Kaplan, E. The receptive field of the primate P retinal ganglion cell, I: Linear dynamics. *Visual Neurosci.* **14**, 169–185 (1997).

[37] VanRullen, R. Perceptual cycles. *Trends Cogn. Sci.* **20**, 723–735 (2016).

[38] Benedetto, A., Spinelli, D. & Morrone, M. C. Rhythmic modulation of visual contrast discrimination triggered by action. *P. R. Soc. Lond. B. Bio.* **283**, 20160692 (2016).

[39] Benedetto, A., Morrone, M. C. & Tomassini, A. The common rhythm of action and perception. *J. Cogn. Neurosci.* **32**, 187–200 (2020).

[40] Kelly, D. H. Motion and vision. II. Stabilized spatio-temporal threshold surface. *J. Opt. Soc. Am.* **69**, 1340–1349 (1979).

[41] Wurtz, R. H. Corollary discharge contributions to perceptual continuity across saccades. *Annu. Rev. Vis. Sci.* **4**, 215–237 (2018).

[42] Schneider, L., Dominguez-Vargas, A.-U., Gibson, L., Kagan, I. & Wilke, M. Eye position signals in the dorsal pulvinar during fixation and goal-directed saccades. *J. Neurophysiol.* **123**, 367–391 (2020).

[43] Masselink, J. & Lappe, M. Visuomotor learning from postdictive motor error. *Elife* **10**, e64278 (2021).

[44] Dowiasch, S., Kaminiarz, A. & Bremmer, F. The visual representation of space in the primate brain. *Neuroforum.* **28**, 199–209 (2022).

[45] Burr, D. C. & Morrone, M. C. The role of neural oscillations in visuo-motor communication at the time of saccades. *Neuropsychologia.* **190**, 108682 (2023).

[46] Rucci, M., Ahissar, E. & Burr, D. Temporal coding of visual space. *Trends Cogn. Sci.* **22**, 883–895 (2018).

[47] Boi, M., Poletti, M., Victor, J. D. & Rucci, M. Consequences of the Oculomotor Cycle for the Dynamics of Perception. *Current Biology* 1–10 (2017).

[48] Yang, B., Intoy, J. & Rucci, M. Eye blinks as a visual processing stage. *Proc. Natl. Acad. Sci. USA* **121**, e2310291121 (2024).

[49] Burr, D. & Ross, J. Contrast sensitivity at high velocities. *Vision Res.* **22** (1982).

[50] Croner, L. J. & Kaplan, E. Receptive fields of P and M ganglion cells across the primate retina. *Vision Res.* **35**, 7–24 (1995).

[51] Xu, X., Anderson, T. J. & Casagrande, V. A. How do functional maps in primary visual cortex vary with eccentricity? *J. Comp. Neurol.* **501**, 741–755 (2007).

[52] Yu, H.-H. *et al.* Spatial and temporal frequency tuning in striate cortex: Functional uniformity and specializations related to receptive field eccentricity. *Eur. J. Neurosci.* **31**, 1043–1062 (2010).

[53] Broderick, W. F., Simoncelli, E. P. & Winawer, J. Mapping spatial frequency preferences across human primary visual cortex. *J. Vis.* **22**, 3 (2022).

[54] Mostofi, N. *et al.* Spatiotemporal content of saccade transients. *Curr. Biol.* **30**, 1–10 (2020).

[55] Roorda, A. Adaptive optics for studying visual function: A comprehensive review. *J. Vis.* **11**, 6 (2011).

[56] Ağaoğlu, M. N., Sheehy, C. K., Tiruveedhula, P., Roorda, A. & Chung, S. T. Suboptimal eye movements for seeing fine details. *J. Vis.* **18**, 8–8 (2018).

[57] Krauzlis, R. J., Goffart, L. & Hafed, Z. M. Neuronal control of fixation and fixational eye movements. *Phil. Trans. R. Soc. B. Biol. Sci.* **372**, 2016205 (2017).

[58] Gruber, L. Z. & Ahissar, E. Closed loop motor-sensory dynamics in human vision. *PLoS ONE* **15**, e0240660 (2020).

[59] de Brouwer, A. J., Flanagan, J. R. & Spering, M. Functional use of eye movements for an acting system. *Trends Cogn. Sci.* **25**, 252–263 (2021).

[60] Leech, J., Gresty, M., Hess, K. & Rudge, P. Gaze failure, drifting eye movements, and centripetal nystagmus in cerebellar disease. *Br. J. Ophthal.* **61**, 774–781 (1977).

[61] Stein, J. & Fowler, M. Unstable binocular control in dyslexic children. *J. Res. Read.* **16**, 30–45 (1993).

[62] Abadi, R. V. Mechanisms underlying nystagmus. *J. R. Soc. Med.* **95**, 231–234 (2002).

[63] Lal, V. & Truong, D. Eye movement abnormalities in movement disorders. *Clin. Park. Relat. Disord.* **1**, 54–63 (2019).

[64] Antoniades, C. A. & Spering, M. Eye movements in Parkinson's disease: From neurophysiological mechanisms to diagnostic tools. *Trends Neurosci.* **47**, 71–83 (2024).

[65] Kumar, G. & Chung, S. T. L. Characteristics of fixational eye movements in people with macular disease. *Invest. Ophthalmol. Vis. Sci.* **55**, 5125–5133 (2014).

[66] Shaikh, A. G., Otero-Millan, J., Kumar, P. & Ghasia, F. F. Abnormal fixational eye movements in amblyopia. *PLoS ONE* **11**, e0149953 (2016).

[67] Ming, W., Palidis, D. J., Spering, M. & McKeown, M. J. Visual contrast sensitivity in early-stage Parkinson's disease. *Invest. Ophthalmol. Vis. Sci.* **57** (2016).

[68] Poletti, M. & Rucci, M. A compact field guide to the study of microsaccades: Challenges and functions. *Vision Res.* **118**, 83–97 (2016).

[69] Hall, J. L. Hybrid adaptive procedure for estimation of psychometric functions. *J. Acoust. Soc. Am.* **69**, 1763–1769 (1981).

[70] Ditchburn, R. W., Fender, D. H. & Mayne, S. Vision with controlled movements of the retinal image. *J. Physiol.* **145**, 98–107 (1959).

[71] Arathorn, D. W., Stevenson, S. B., Yang, Q., Tiruveedhula, P. & Roorda, A. How the unstable eye sees a stable and moving world. *J. Vis.* **13** (2013).

[72] Wichmann, F. A. & Hill, N. J. The psychometric function : I . Fitting , sampling , and goodness of fit. *Percept. Psychophys.* **63**, 1293–1313 (2001).

[73] Engbert, R. & Kliegl, R. Microsaccades keep the eyes' balance during fixation. *Psychol. Sci.* **15**, 431–436 (2004).

[74] Engbert, R., Mergenthaler, K., Sinn, P. & Pikovsky, A. An integrated model of fixational eye movements and microsaccades. *Proc. Natl. Acad. Sci. USA* **108**, 765–770 (2011).

[75] Victor, J. D. The dynamics of the cat retinal X cell center. *J. Physiol.* **386**, 219–46 (1987).